

# Pseudo Jahn-Teller Effect and Magnetoelastic Coupling in Spin-Orbit Mott Insulators

Huimei Liu and Giniyat Khaliullin

Max Planck Institute for Solid State Research, Heisenbergstrasse 1, D-70569 Stuttgart, Germany

(Dated: June 4, 2022)

The consequences of the Jahn-Teller (JT) orbital-lattice coupling for magnetism of pseudospin  $J_{\text{eff}} = 1/2$  and  $J_{\text{eff}} = 0$  compounds are addressed. In the former case, represented by  $\text{Sr}_2\text{IrO}_4$ , this coupling generates, through the so-called pseudo-JT effect, orthorhombic deformations of a crystal concomitant with magnetic ordering. The orthorhombicity axis is tied to the magnetization and rotates with it under magnetic field. The theory resolves a number of puzzles in  $\text{Sr}_2\text{IrO}_4$  such as the origin of in-plane magnetic anisotropy and magnon gaps, metamagnetic transition, etc. In  $J_{\text{eff}} = 0$  systems, the pseudo-JT effect leads to spin-nematic transition well above magnetic ordering, which may explain the origin of “orbital order” in  $\text{Ca}_2\text{RuO}_4$ .

Electron-phonon coupling leads to a wide range of phenomena, from Cooper pairing in metals to Jahn-Teller effect in Mott insulators. The Jahn-Teller (JT) effect, arising from coupling of the orbital degrees of freedom of localized electrons to lattice vibrations (“orbital-lattice coupling”), is a major source driving structural phase transitions. Below the JT structural transition temperature  $T_{\text{JT}}$ , the orbital fluctuations are quenched, and resulting orbital order dictates the spin-exchange couplings  $J$  and magnetic structure below  $T_m$  via so-called Goodenough-Kanamori rules [1, 2]. Typically, the JT and magnetic transitions are well separated; a canonical example is  $\text{LaMnO}_3$  with  $T_{\text{JT}} \sim 800$  K and  $T_m \sim 140$  K.

The picture of successive orbital and spin orderings, and associated Goodenough-Kanamori rules that guided spin-orbital physics in transition metal compounds over decades, are based on a spin-orbital separation idea assuming distinct energy scales and excitations in spin and orbital sectors. Recently, materials based on late transition metal ions with strong spin-orbit coupling (SOC) came into focus. In these compounds, spin-orbital separation is no longer at work, and both magnetism and JT physics have to be reformulated in terms of “pseudospins” [3], or “effective spins”  $J_{\text{eff}}$  [4], corresponding (but not always) to the total angular momentum. While the pseudospin magnetism, especially in  $J_{\text{eff}} = 1/2$  systems, is now well understood (see the recent reviews [5–9]), the JT physics in spin-orbit Mott insulators remains largely unexplored. Partially, this is due to common belief that JT coupling in  $J_{\text{eff}} = 1/2$  systems is not essential at all, since it cannot split the Kramers doublet.

In this Letter, we show that JT coupling has in fact a decisive impact on low-energy magnetic properties of  $J_{\text{eff}} = 1/2$ , and even nominally nonmagnetic  $J_{\text{eff}} = 0$ , compounds. By virtue of the pseudo-JT effect [10–12], orbital-lattice coupling modulates the spatial shape of the pseudospin wavefunction and generates new terms in the Hamiltonian, describing the pseudospin-lattice coupling. Albeit weak, these terms lead to the qualitative effects: in  $J_{\text{eff}} = 1/2$  system  $\text{Sr}_2\text{IrO}_4$ , we predict that they induce the tetragonal-to-orthorhombic structural transition, which turns out to be instrumental for understand-

ing the magnetic properties of this compound, including metamagnetic behavior, the origin of magnon gaps, etc. In  $J_{\text{eff}} = 0$  systems, the JT coupling results in a simultaneous lattice and spin-rotational symmetry breaking transition well above  $T_m$ .

*Pseudospin-lattice coupling,  $J_{\text{eff}} = 1/2$ .*— While physical ideas are generic to a broad class of spin-orbit Mott insulators [5–9, 13, 14], we focus here on  $\text{Sr}_2\text{IrO}_4$ , which is of special interest due to its quasi-two-dimensional (2D) antiferromagnetism (AF) [15] and magnon excitations [16] similar to those of  $\text{La}_2\text{CuO}_4$  [17].

The JT interaction operates in a quadrupolar channel, i.e. it couples lattice deformations  $\varepsilon_\gamma$  of certain symmetry  $\gamma$  to the orbital quadrupolar moments  $Q^\gamma$  of valence electrons:  $\mathcal{H}_{\text{JT}} \propto g_\gamma \varepsilon_\gamma Q^\gamma$ . Through the spin-orbit entanglement, this coupling should generate pseudospin-lattice coupling  $\mathcal{H}_{\text{s-l}}$  of the same form, with  $Q^\gamma$  replaced by the pseudospin quadrupoles  $Q_s^\gamma$ . As no single-ion quadrupole can be formed out of pseudospin  $S = 1/2$ ,  $Q_s^\gamma$  should involve at least two sites, i.e. bilinear forms  $S_i^\alpha S_j^\beta$  of a proper symmetry, suggesting a minimal coupling  $\mathcal{H}_{\text{s-l}}^{ij} \propto \tilde{g}_\gamma \varepsilon_\gamma Q_s^\gamma(ij)$ . Below, we derive this interaction and evaluate the coupling constants  $\tilde{g}_\gamma$ .

We consider the orthorhombic deformations which are most common in perovskites. In a tetragonal  $\text{Sr}_2\text{IrO}_4$ , these are  $xy$  and  $x^2-y^2$  type distortions, which we quantify by  $\varepsilon_1 = \frac{b-a}{b+a}$  and  $\varepsilon_2 = \frac{x-y}{x+y}$ , correspondingly, using the coordinate frames of Fig. 1.  $\varepsilon_1$  and  $\varepsilon_2$  measure elongation of a crystal along  $b$  and  $x$  directions, respectively. The distortions split  $t_{2g}$  level via the JT coupling:

$$\mathcal{H}_{\text{JT}} = g_1 \varepsilon_1 (n_{az} - n_{bz}) + g_2 \varepsilon_2 (n_{zx} - n_{yz}). \quad (1)$$

This coupling mixes the Kramers doublets  $A$  and  $B$  of  $\text{Ir}^{4+}$  ion (Fig. 1), resulting in the “orthorhombically distorted” pseudospin wavefunction  $\tilde{A}$ :

$$|\tilde{A}_\pm\rangle = \frac{1}{\sqrt{1+|\eta_\pm|^2}} (|A_\pm\rangle + \eta_\pm |B_\mp\rangle), \quad (2)$$

where  $\eta_\pm = \frac{\cos\theta}{E_{BA}}(\pm i g_1 \varepsilon_1 + g_2 \varepsilon_2)$ . The angle  $\theta$  with  $\tan 2\theta = 2\sqrt{2}\lambda/(\lambda + 2\Delta)$  quantifies a tetragonal field  $\Delta$  relative to SOC constant  $\lambda$ , and  $E_{BA} \sim \frac{3}{2}\lambda$  is the energy

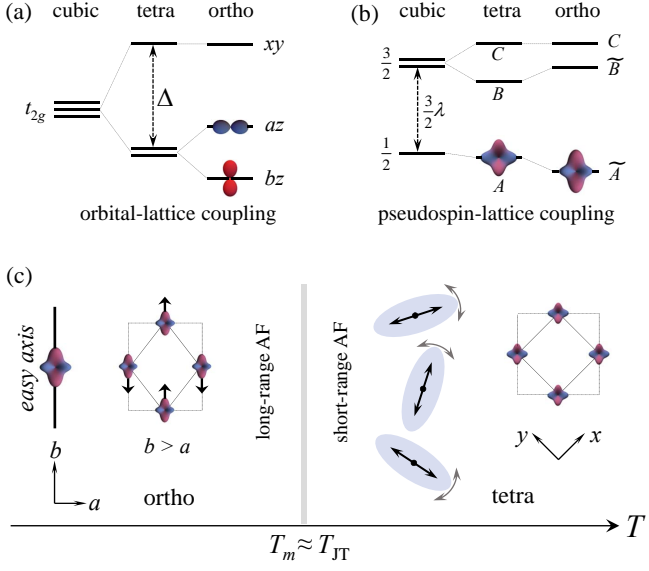


FIG. 1:  $t_{2g}$ -hole level structure (a) without and (b) with SOC under cubic, tetragonal, and orthorhombic crystal fields. Elongation of a crystal along the  $b$ -axis ( $\varepsilon_1$  deformation) splits  $az = \frac{1}{\sqrt{2}}(x - y)z$  (blue) and  $bz = \frac{1}{\sqrt{2}}(x + y)z$  (red) orbitals. This enhances the  $bz$ -component of the ground state wavefunction  $\tilde{A}$ , breaking its tetragonal symmetry (top view;  $xy$  orbital is not shown for clarity). (c) Illustration of the magnetoelastic coupling in  $\text{Sr}_2\text{IrO}_4$ . Above the structural transition at  $T_{JT} \approx T_m$ , symmetry is tetragonal on average, but slowly rotating domains of the orthorhombic distortions and quasi-2D magnetism develop. Below  $T_{JT}$ , the tetragonal symmetry is broken, selecting  $b$  axis for the moment direction.

difference between  $A$  and  $B$  levels. The “tetragonal”, i.e. unperturbed wavefunctions  $|A_{\pm}\rangle = \sin\theta|0, \pm\frac{1}{2}\rangle - \cos\theta|\pm 1, \mp\frac{1}{2}\rangle$  and  $|B_{\pm}\rangle = |\pm 1, \pm\frac{1}{2}\rangle$ , in terms of  $t_{2g}$  orbital and spin quantum numbers.

Next, we inspect how the shape-distortions of the ground state wavefunction  $\tilde{A}$  affect the pseudospin interactions. Deformations are assumed to be quasi-static (adiabatic approximation). Projecting the Kugel-Khomskii type spin-orbital Hamiltonian, Eq. (3.11) of Ref. [3], onto  $\tilde{A}$  subspace, we find  $\mathcal{H} = \mathcal{H}_s + \mathcal{H}_{s-1}$ .  $\mathcal{H}_s$  comprises the nearest-neighbor Heisenberg  $J$ , Ising  $J_z$ , Dzyaloshinskii-Moriya  $D$ , and pseudodipolar  $K$  terms

$$J\vec{S}_i \cdot \vec{S}_j + J_z S_i^z S_j^z + \vec{D} \cdot [\vec{S}_i \times \vec{S}_j] + K(\vec{S}_i \cdot \vec{r}_{ij})(\vec{S}_j \cdot \vec{r}_{ij}) \quad (3)$$

derived earlier [18], while

$$\mathcal{H}_{s-1}^{ij} = \tilde{g}_1 \varepsilon_1 (S_i^x S_j^y + S_i^y S_j^x) + \tilde{g}_2 \varepsilon_2 (S_i^x S_j^x - S_i^y S_j^y) \quad (4)$$

constitutes the (pseudo)spin-lattice interaction that we are looking for. It linearly couples the spin quadrupoles  $Q_s^1$  and  $Q_s^2$  of  $xy$  and  $x^2 - y^2$  symmetries to corresponding lattice deformations. In essence,  $\mathcal{H}_{s-1}$  is nothing but  $\mathcal{H}_{JT}$  “reincarnated” as a spin-lattice coupling in  $J_{\text{eff}} = 1/2$  insulator. The coupling constants  $\tilde{g}$  are renormalized from

Eq. 1 to  $\tilde{g} = \kappa g$  by  $\kappa \simeq \frac{t^2 \sin^2 2\theta}{U E_{BA}}$ , where  $t$ ,  $U$ , and  $J_H$  are hopping amplitude, Coulomb repulsion, and Hund’s coupling, respectively. Roughly, we estimate  $\kappa \sim 5 \times 10^{-3}$  and hence  $\tilde{g} \sim 25$  meV in  $\text{Sr}_2\text{IrO}_4$ , using  $g \sim 5$  eV typical for  $t_{2g}$  systems. In  $J_{\text{eff}} = 1/2$  compounds based on  $4d$   $\text{Ru}^{3+}$  and  $3d$   $\text{Co}^{2+}$  ions,  $\kappa$  and  $\tilde{g}$  should increase as  $1/\lambda$ .

*Breaking tetragonal symmetry.*— Having derived spin-lattice interaction  $\mathcal{H}_{s-1}$ , we discuss now its consequences for low-energy properties of  $\text{Sr}_2\text{IrO}_4$ . First of all, just as the JT coupling, it should lead to the structural instability as soon as the spin quadrupolar moments  $Q_s^{\gamma}$  develop within the (quasi) long-range ordered magnetic domains. Denoting the staggered moment direction by  $\alpha$ ,  $\vec{n} = S(\cos\alpha, \sin\alpha)$ , we find  $\langle Q_s^1 \rangle = -S^2 \sin 2\alpha$  and  $\langle Q_s^2 \rangle = -S^2 \cos 2\alpha$  per bond. From Eq. 4 and elastic energy  $\frac{1}{2}K_{\gamma}\varepsilon_{\gamma}^2$ , the spin-lattice induced orthorhombic deformations follow:

$$\langle \varepsilon_1 \rangle = \frac{\Gamma_1}{\tilde{g}_1} \sin 2\alpha, \quad \langle \varepsilon_2 \rangle = \frac{\Gamma_2}{\tilde{g}_2} \cos 2\alpha, \quad (5)$$

where  $\Gamma_{\gamma} = 2S^2 \tilde{g}_{\gamma}^2 / K_{\gamma}$ . A mean-field part of  $\mathcal{H}_{s-1}$  (4) reads then as follows:

$$\Gamma_1 \sin 2\alpha (S_i^x S_j^y + S_i^y S_j^x) + \Gamma_2 \cos 2\alpha (S_i^x S_j^x - S_i^y S_j^y), \quad (6)$$

with  $\alpha$  to be obtained by minimizing the ground state energy  $E(\alpha)$ . Classically,  $E(\alpha) = \text{const} + S^2(\Gamma_1 - \Gamma_2) \cos^2 2\alpha$ . For  $\Gamma_1 > \Gamma_2$ ,  $E(\alpha)$  is minimized at  $\alpha = 45^\circ$ , which is exactly the case of  $\text{Sr}_2\text{IrO}_4$  [15, 19]. Our theory predicts then  $\varepsilon_1$ -type ( $b > a$ ) orthorhombic distortion, as depicted in Fig. 1(c). This type of distortion is natural for perovskites, as it does not affect the Me-O-Me bond length.

Breaking  $C_4$  symmetry by spin-lattice coupling opens the in-plane magnon gap already on a level of linear spin-wave theory. Eqs. 3 and 6 give  $\omega_{ab} \simeq 8S\sqrt{J\Gamma_1}$ . With  $\omega_{ab} \sim 2.1 - 2.4$  meV [20, 21] and  $J \sim 100$  meV [16, 22], we evaluate  $\Gamma_1 \sim 3$   $\mu\text{eV}$ . Eq. 5 predicts then the spin-lattice induced distortion of the order of  $\varepsilon_1 \sim 10^{-4}$  [23]. The two-fold  $C_2$  anisotropy of magnetoresistivity [26] and the signatures of orthorhombic distortions [27, 28] in  $\text{Sr}_2\text{IrO}_4$  find a natural explanation within our theory. Future experiments using, e.g., Larmor diffraction [29] should be able to quantify  $\varepsilon_1$  directly. We note also that the deformation induced magnon gap  $\omega_{ab}$  far exceeds interlayer couplings [30], and should therefore be essential for establishing the magnetic order at high  $T_m \sim 240$  K.

To summarize up to now, the combined action of spin-orbit and JT couplings results in the interaction between magnetic quadrupoles and lattice deformation. Dynamically, coupled oscillations of the  $\vec{n}$ -moment direction and lattice vibrations (magnetoacoustic effects [31, 32]) are expected; this is an interesting topic for future research. Most importantly, a structural instability is inevitable no matter how large SOC is; this invalidates a common assertion that high tetragonal symmetry of  $J_{\text{eff}} = 1/2$  system  $\text{Sr}_2\text{IrO}_4$  is protected by large SOC.

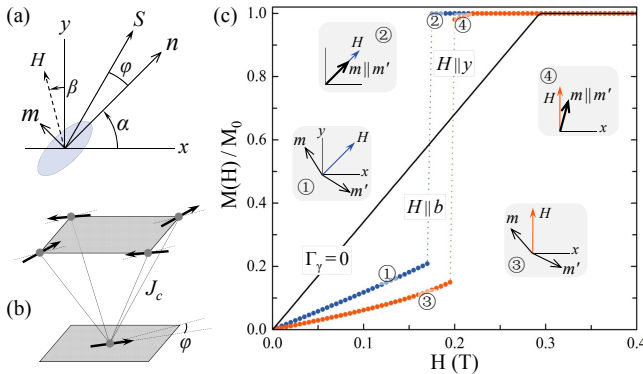


FIG. 2: Schematic of (a) staggered  $\vec{n}$  and canted  $\vec{m}$  moments, magnetic field  $H$ , and spin-lattice induced orthorhombic deformation (shaded ellipse), and (b) interlayer AF coupling  $J_c$  between spins. (c) Magnetization curves for a magnetic field applied along the "easy" ( $H \parallel b$ ) and "hard" ( $H \parallel y$ ) axes. While the magnetization  $\vec{M} \propto \vec{m} + \vec{m}'$  grows linearly with  $H$  when  $\Gamma_\gamma = 0$ , a metamagnetic transition caused by magnetoelastic coupling is observed at finite  $\Gamma_\gamma$  (we used  $\Gamma_1 = 3 \mu\text{eV}$  and  $\Gamma_2 = 0.6\Gamma_1$ ). Insets depict the mutual orientation of  $\vec{m}$  and  $\vec{m}'$  moments on different layers at representative points on the  $M(H)$  curves.

*Metamagnetic transition, in-plane magnon gap.*— We discuss now further manifestations of magnetoelastic coupling in  $\text{Sr}_2\text{IrO}_4$ . Via spin-lattice coupling, the reorientations of moments under external magnetic field will affect lattice deformations. The latter, in turn, modifies the magnetic anisotropy potential. Such feedback effects result in a non-monotonic behavior of magnetization  $M(H)$ . In  $\text{Sr}_2\text{IrO}_4$ , spins are canted by angle  $\varphi \simeq D/2J \sim 12^\circ$  [33], see Fig. 2(a,b). Magnetic field couples to the canted moments  $\vec{m}$ . To calculate  $M(H)$ , we use a simple model in Fig. 2(b) for the interlayer coupling. The total energy  $E$  depends now on two angles  $\alpha$  and  $\alpha'$ , corresponding to the moment directions in different layers, and the field direction  $\beta$ . We find  $E(\alpha, \alpha', \beta) = \text{const} + \frac{S}{2}F$ , with

$$F = \sin \varphi [h_c \cos(\alpha - \alpha') - h \cos(\alpha - \beta) - h \cos(\alpha' - \beta)] - \frac{S}{2} [\Gamma_1 (\sin 2\alpha + \sin 2\alpha')^2 + \Gamma_2 (\cos 2\alpha + \cos 2\alpha')^2]. \quad (7)$$

Here,  $h = g\mu_B H$ , and  $h_c = 4J_c S \sin \varphi$  is the interlayer field. Minimization of  $F$  gives  $\alpha$  and  $\alpha'$  as a function of  $\vec{H}$ , from which the canted moments  $\vec{m}$  and  $\vec{m}'$  on different planes and total magnetization  $\vec{M}$  follow. The deformations  $\varepsilon_1$  and  $\varepsilon_2$  are given by Eq. 5, where  $\sin 2\alpha$  and  $\cos 2\alpha$  replaced now by  $\frac{1}{2}(\sin 2\alpha + \sin 2\alpha')$  and  $\frac{1}{2}(\cos 2\alpha + \cos 2\alpha')$ , respectively; this implies the field-dependence of the deformations (magnetostriction).

Fig. 2(c) shows  $M(H)/M_0$  calculated with  $h_c = 18 \mu\text{eV}$  ( $\simeq 0.16$  T). Without spin-lattice coupling,  $\vec{m}$  and  $\vec{m}'$  gradually rotate towards each other and  $M$  grows monotonically. Spin-lattice induced anisotropy results

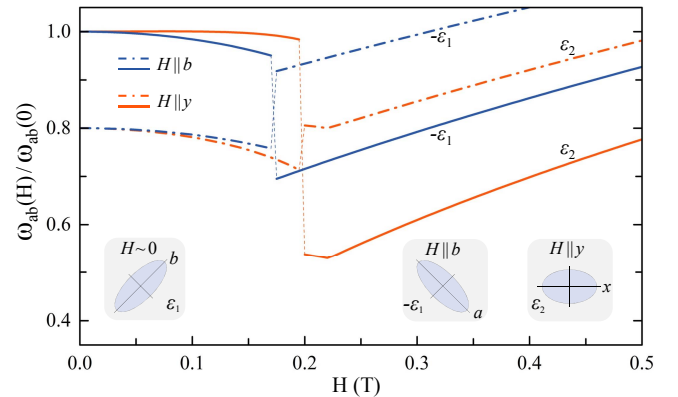


FIG. 3: Magnon gaps as a function of magnetic field along  $b$  ([010] in orthorhombic notation, blue) and  $y$  ([110], red) directions. Dash-dotted (solid) line corresponds to the in-phase (anti-phase) rotations of  $\vec{m}$  and  $\vec{m}'$  moments. At small  $H$ , the distortion is of  $\varepsilon_1$  symmetry. At large  $H$ , it remains  $\varepsilon_1$ -type for  $H \parallel b$ . For  $H \parallel y$ , the deformation changes from large  $\varepsilon_1$  to small  $\varepsilon_2$ , resulting in a drop of the anisotropy energy and  $\omega_{ab}$ . The parameters are as in Fig. 2.

in a metamagnetic transition as observed [15, 19]. At  $H = H_{cr}$ ,  $\vec{m}$  and  $\vec{m}'$  flip and become parallel. For  $\Gamma_1 > \Gamma_2$  as in  $\text{Sr}_2\text{IrO}_4$ ,  $H_{cr}$  for easy-axis  $b$  is lower than that for hard-axis; this result has recently been confirmed experimentally [34]. We note that  $M(H)$  near  $H_{cr}$  is sensitive to angle  $\beta$ , so the quenched disorder and sample alignment issues should be relevant in the data analysis.

Next, we discuss the in-plane magnon gaps generated by spin-lattice coupling  $\mathcal{H}_{s-1}$ . Due to interlayer coupling, there are two different modes. At small fields,  $H \ll H_{cr}$ , the optical and acoustic mode gaps are  $8S\sqrt{J(\Gamma_1 + \frac{\sin \varphi}{8S}h_c)}$  and  $8S\sqrt{J\Gamma_1}$ , respectively. Above the metamagnetic transition,  $H \geq H_{cr}$ , we find

$$\omega_{ab}^\pm \simeq 8S\sqrt{J\{\Gamma(\alpha) + \frac{\sin \varphi}{8S}[h \cos(\alpha - \beta) - h_c \pm h_c]\}}. \quad (8)$$

Here,  $\Gamma(\alpha) = \Gamma_1 \sin^2 2\alpha + \Gamma_2 \cos^2 2\alpha$ , and  $\alpha$  follows from  $2S(\Gamma_1 - \Gamma_2) \sin 4\alpha = h \sin \varphi \sin(\alpha - \beta)$ . For  $H \parallel b$ , this gives  $\alpha = \beta$  ( $= -\frac{\pi}{4}$ ) and  $\Gamma(\alpha) = \Gamma_1$ . For  $H \parallel y$  along  $y$  axis,  $\alpha \sim \beta$  ( $= 0$ ) and thus  $\Gamma(\alpha) \sim \Gamma_2$ ; this implies weak distortion  $\varepsilon_2$  and smaller magnon gap. The main message is that the magnon gaps become strongly dependent on the field direction, as shown in Fig. 3. The above equations should help to quantify  $\Gamma_1$  and  $\Gamma_2$  from experiments. The results in Fig. 3 are qualitatively consistent with the recent Raman data [20]; a detailed analysis would require a derivation of the Raman matrix elements necessary for the mode assignment.

Via the magnetoelastic coupling, quasi-2D AF correlations above  $T_m$  [22, 35] should lead to slowly fluctuating lattice deformations (see Fig. 1) which, in turn, will affect phonon dynamics. Indeed, strong Fano anomalies of phonons have been observed in  $\text{Sr}_2\text{IrO}_4$  [36].

*Spin-nematic order in  $J_{\text{eff}} = 0$  systems.*— Finally, we move to pseudospin  $J_{\text{eff}} = 0$  case, and show that, despite having neither orbital nor spin degeneracy, the JT coupling is relevant even here. In general, the  $J_{\text{eff}} = 0$  compounds are of interest because they host "excitonic" magnetism [37] - magnetic order via condensation of spin-orbit  $J_{\text{eff}} = 0 \rightarrow 1$  excitations. The expected non-Heisenberg type magnon and amplitude (Higgs) modes have been observed in  $\text{Ca}_2\text{RuO}_4$  [38, 39]. Also,  $J_{\text{eff}} = 0$  systems illustrate well the interplay between three "grand forces" in Mott insulators - the JT coupling, spin-orbital exchange interaction, and spin-orbit coupling [3].

As a toy model, we consider 2D square lattice of  $J_{\text{eff}} = 0$  ions (e.g.,  $d^4$   $\text{Ru}^{4+}$ ) in an octahedral field. The  $t_{2g}^4$  orbital configuration is subject to the JT effect; however, it is opposed by SOC that favors spin-orbit singlet  $J_{\text{eff}} = 0$  instead [37, 40]. This competition can be resolved by mixing the  $J_{\text{eff}} = 0$  wavefunction with the excited  $J_{\text{eff}} = 1$  states, by virtue of spin-orbital exchange interactions. Since  $J_{\text{eff}} = 1$  level hosts a quadrupolar moment, the ground state becomes JT active, and the phase transition, breaking simultaneously the lattice and spin-rotational symmetries, may develop. In essence, this is the "spin nematic" phase discussed in the context of large  $J_{\text{eff}}$  systems [41], but with the quadrupolar order parameter depending now on the  $J_{\text{eff}} = 1$  fraction in the condensate.

A minimal model for  $d^4$  system can be cast in terms of hard-core bosons  $\mathbf{T} = (T_x, T_y, T_z)$ , describing excitations from the ground state  $J_{\text{eff}} = 0$  singlet to  $J_{\text{eff}} = 1$  triplet. The spin-orbit  $\lambda$  and exchange  $J \simeq 4t^2/U$  couplings read then as follows [37]:

$$\mathcal{H}_{\lambda, J} = \lambda \sum_i n_i^T + J \sum_{\langle ij \rangle} \frac{1}{4} (\mathbf{T}_i^\dagger \cdot \mathbf{T}_j - \mathbf{T}_i \cdot \mathbf{T}_j + H.c.). \quad (9)$$

Regarding the JT coupling, we consider a tetragonal distortion  $\varepsilon = \frac{a+b-2c}{a+b+c}$ , which splits the  $xy$  and  $xz/yz$  orbital levels by  $g\varepsilon$ :  $\mathcal{H}_{\text{JT}} = g\varepsilon \frac{1}{3}(n_{xz} + n_{yz} - 2n_{xy})$ . In the spin-orbit entangled  $T$ -basis, this coupling lowers  $J_{\text{eff}} = 0$  singlet by  $E_s = (\frac{3}{2} - \frac{\delta}{3} - \sqrt{\frac{9}{4} - \delta + \delta^2})\lambda$ , and splits  $J_{\text{eff}} = 1$  triplet into  $T_{x/y}$  doublet and  $T_z$  singlet by  $\Delta_z = (\delta + \sqrt{1 + \delta^2} - 1)\lambda$ , where  $\delta = g\varepsilon/2\lambda$ . As a result, the spin gap reduces from  $\lambda$  to  $E = (\frac{1}{2} + \sqrt{\frac{9}{4} - \delta + \delta^2 - \sqrt{1 + \delta^2}})\lambda$ , see Fig. 4(a). At the critical value of  $E \sim J$ , the  $T_{x/y}$  doublet condenses, forming a ground state with finite quadrupole moment  $Q = n_x^T + n_y^T - 2n_z^T$ . While the cubic symmetry may be broken at finite temperature  $T_{\text{JT}}$ , long-range magnetic order is delayed due to  $XY$ -type phase fluctuations; therefore,  $T_m$  and  $T_{\text{JT}}$  are separated in quasi-2D  $J_{\text{eff}} = 0$  systems. We think that the "orbital order" in  $\text{Ca}_2\text{RuO}_4$  near 260 K [42], well above  $T_m$ , is in fact the JT driven spin-nematic order. The observed  $XY$ -type magnons [38] further support the picture of spin-orbit entangled  $T_{x/y}$  condensate.

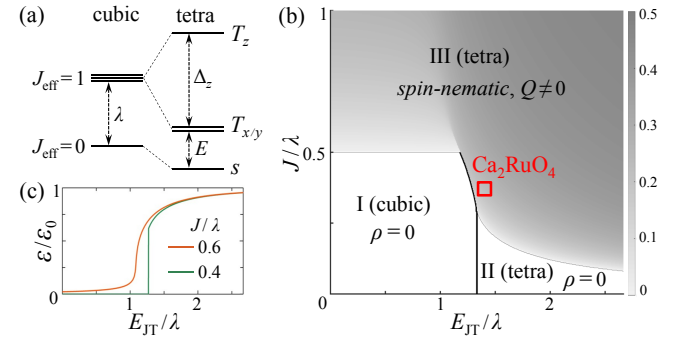


FIG. 4: (a) Singlet-triplet level structure under tetragonal JT distortion. (b) Phase diagram of  $J_{\text{eff}} = 0$  system. Small  $J$  area contains two nonmagnetic phases separated by a first order transition (thick line). In phase I, the JT effect is fully suppressed, while phase II is tetragonally distorted. As  $J$  increases, the exchange interactions promote condensation of the  $T_{x/y}$  states, forming spin nematic phase with nonzero  $Q$  moment (quantified by color intensity) and  $XY$ -type magnetism. (c) Lattice distortion  $\varepsilon$  relative to its value at  $\lambda = 0$ .

A mean-field phase diagram of  $\mathcal{H}_{\lambda, J} + \mathcal{H}_{\text{JT}}$ , supplemented by the elastic energy  $\frac{1}{2}K\varepsilon^2$ , is shown in Fig. 4(b) as a function of  $J/\lambda$  and  $E_{\text{JT}}/\lambda$ .  $E_{\text{JT}} = \Delta/3$  is the JT stabilization energy, where  $\Delta = \frac{2g^2}{3K}$  is the  $t_{2g}$  orbital splitting at  $\lambda = 0$ . At small  $J$  and  $E_{\text{JT}}$ , SOC imposes the  $J_{\text{eff}} = 0$  phase I; at large  $E_{\text{JT}}$ , it gives way to the JT-distorted nonmagnetic phase II with finite spin-gap  $E$ . In phase III, stabilized by a combined action of the exchange and JT couplings,  $XY$ -type magnetic condensate is formed.

Interestingly, the observed magnon bandwidth  $\sim 2J \sim 50$  meV [38] and ratio  $\Delta/2\lambda \sim 2$  [43, 44] locate  $\text{Ca}_2\text{RuO}_4$  in the critical area of the phase diagram [see Fig. 4(b)]. This suggests that an unusual magnetism [38, 39] and extreme sensitivity of  $\text{Ca}_2\text{RuO}_4$  to external perturbations [45, 46] are caused by frustration among the JT, spin-orbit, and exchange interactions, further boosted by its proximity to metal-insulator transition.

To conclude, in contrast to the common wisdom, the JT coupling remains an essential part of the low-energy physics in spin-orbit  $J_{\text{eff}} = 1/2$ , and even  $J_{\text{eff}} = 0$ , Mott insulators. Converted into pseudospin-lattice coupling via spin-orbit entanglement, it leads to the structural transitions and magnetoelastic effects. We have shown that the JT coupling resolves hitherto unexplained puzzles of  $J_{\text{eff}} = 1/2$   $\text{Sr}_2\text{IrO}_4$ , and is essential for the phase behavior of  $J_{\text{eff}} = 0$   $\text{Ca}_2\text{RuO}_4$ . This leads us to believe that pseudospin-lattice coupling should be generic to a broad class of spin-orbit  $J_{\text{eff}}$  compounds, including the Kitaev-model materials of high current interest [5–8]. In the latter, the pseudospins are highly frustrated, and their coupling to lattice may lead to more radical effects than in conventional, unfrustrated magnets like  $\text{Sr}_2\text{IrO}_4$ .

We thank B. J. Kim, J. Porras, J. Bertinshaw, B. Keimer, J. Chaloupka, and O. P. Sushkov for discussions. We acknowledge support by the European Research Council under Advanced Grant No. 669550 (Com4Com).

---

[1] J. B. Goodenough, *Magnetism and the Chemical Bond* (Interscience Publ., New York, 1963).

[2] K. I. Kugel and D. I. Khomskii, Sov. Phys. Usp. **25**, 231 (1982).

[3] G. Khaliullin, Prog. Theor. Phys. Suppl. **160**, 155 (2005).

[4] B. J. Kim, Hosub Jin, S. J. Moon, J.-Y. Kim, B.-G. Park, C. S. Leem, Jaejun Yu, T. W. Noh, C. Kim, S.-J. Oh, J.-H. Park, V. Durairaj, G. Cao, and E. Rotenberg, Phys. Rev. Lett. **101**, 076402 (2008).

[5] J. G. Rau, E. K.-H. Lee, and H.-Y. Kee, Annu. Rev. Condens. Matter Phys. **7**, 195 (2016).

[6] S. M. Winter, A. A. Tsirlin, M. Daghofer, J. van den Brink, Y. Singh, P. Gegenwart, and R. Valentí, J. Phys.: Condens. Matter **29**, 493002 (2017).

[7] S. Trebst, *Lecture notes of the 48th IFF Spring School "Topological Matter"* (2017) arXiv:1701.07056.

[8] M. Hermanns, I. Kimchi, J. Knolle, Annu. Rev. Condens. Matter Phys. **9**, 17 (2018).

[9] J. Bertinshaw, Y.K. Kim, G. Khaliullin, and B.J. Kim. Annu. Rev. Condens. Matter Phys. (in press).

[10] The pseudo-JT effect is an extension of the JT effect to systems with orbital-singlet ground states; it operates through the mixing of the ground and excited states under the nuclear displacements [11, 12].

[11] I. B. Bersuker, Chem. Rev. **113**, 1351 (2013).

[12] I. B. Bersuker, *The Jahn-Teller effect* (Cambridge University Press, Cambridge, 2006).

[13] H. Liu and G. Khaliullin, Phys. Rev. B **97**, 014407 (2018).

[14] R. Sano, Y. Kato, and Y. Motome, Phys. Rev. B **97**, 014408 (2018).

[15] B. J. Kim, H. Ohsumi, T. Komesu, S. Sakai, T. Morita, H. Takagi, and T. Arima, Science **323**, 1329 (2009).

[16] J. Kim, D. Casa, M. H. Upton, T. Gog, Y.-J. Kim, J. F. Mitchell, M. van Veenendaal, M. Daghofer, J. van den Brink, G. Khaliullin, and B. J. Kim, Phys. Rev. Lett. **108**, 177003 (2012).

[17] See Ref. [9] for an extensive discussion of the analogy between iridates and cuprates.

[18] G. Jackeli and G. Khaliullin, Phys. Rev. Lett. **102**, 017205 (2009).

[19] G. Cao, J. Bolivar, S. McCall, J. E. Crow, and R. P. Guertin, Phys. Rev. B **57**, R11039 (1998).

[20] Y. Gim, A. Sethi, Q. Zhao, J. F. Mitchell, G. Cao, and S. L. Cooper, Phys. Rev. B **93**, 024405 (2016).

[21] H. Gretarsson, J. Sauceda, N. H. Sung, M. Höppner, M. Minola, B. J. Kim, B. Keimer, and M. Le Tacon, Phys. Rev. B **96**, 115138 (2017).

[22] S. Fujiyama, H. Ohsumi, T. Komesu, J. Matsuno, B. J. Kim, M. Takata, T. Arima, and H. Takagi, Phys. Rev. Lett. **108**, 247212 (2012).

[23] We recall that  $\varepsilon \propto \tilde{g} \propto 1/\lambda$ . In pseudospin-1/2  $\text{Co}^{2+}$  compounds, where  $\lambda$  is one order of value smaller than in iridates, magnetic order induced distortions should be of the order of  $10^{-3}$ , as indeed observed [24, 25].

[24] A. Okazaki and Y. Suemune, J. Phys. Soc. Jpn. **16**, 671 (1961).

[25] N. C. Tombs and H. P. Rooksby, Nature **165**, 442 (1950).

[26] C. Wang, H. Seinige, G. Cao, J.-S. Zhou, J. B. Goodenough, and M. Tsoi, J. Appl. Phys. **117**, 17A310 (2015).

[27] C. Dhital, T. Hogan, Z. Yamani, C. de la Cruz, X. Chen, S. Khadka, Z. Ren, and S. D. Wilson, Phys. Rev. B **87**, 144405 (2013).

[28] F. Ye, S. Chi, B. C. Chakoumakos, J. A. Fernandez-Baca, T. Qi, and G. Cao, Phys. Rev. B **87**, 140406(R) (2013).

[29] B. Náfrádi, T. Keller, F. Hardy, C. Meingast, A. Erb, and B. Keimer, Phys. Rev. Lett. **116**, 047001 (2016).

[30] T. Takayama, A. Matsumoto, G. Jackeli, and H. Takagi, Phys. Rev. B **94**, 224420 (2016).

[31] C. Kittel, Phys. Rev. **110**, 836 (1958).

[32] E. A. Turov and V. G. Shavrov, Sov. Phys. Usp. **26**, 593 (1983).

[33] S. Boseggia, H. C. Walker, J. Vale, R. Springell, Z. Feng, R. S. Perry, M. Moretti Sala, H. M. Rønnow, S. P. Collins, and D. F. McMorrow, J. Phys.: Condens. Matter **25**, 422202 (2013).

[34] J. Porras, J. Bertinshaw, H. Liu, G. Khaliullin, N. H. Sung, J.-W. Kim, S. Francoual, P. Steffens, G. Deng, A. Said, D. Casa, X. Huang, T. Gog, J. Kim, B. Keimer, and B. J. Kim, arXiv:1808.\*\*\*\*\*.

[35] J. G. Vale, S. Boseggia, H. C. Walker, R. Springell, Z. Feng, E. C. Hunter, R. S. Perry, D. Prabhakaran, A. T. Boothroyd, S. P. Collins, H. M. Rønnow, and D. F. McMorrow, Phys. Rev. B **92**, 020406(R) (2015).

[36] H. Gretarsson, N. H. Sung, M. Höppner, B. J. Kim, B. Keimer, and M. Le Tacon, Phys. Rev. Lett. **116**, 136401 (2016).

[37] G. Khaliullin, Phys. Rev. Lett. **111**, 197201 (2013).

[38] A. Jain, M. Krautloher, J. Porras, G. H. Ryu, D. P. Chen, D. L. Abernathy, J. T. Park, A. Ivanov, J. Chaloupka, G. Khaliullin, B. Keimer, and B. J. Kim, Nat. Phys. **13**, 633 (2017).

[39] S. M. Souliou, J. Chaloupka, G. Khaliullin, G. Ryu, A. Jain, B. J. Kim, M. Le Tacon, and B. Keimer, Phys. Rev. Lett. **119**, 067201 (2017).

[40] O. N. Meetei, W. S. Cole, M. Randeria, and N. Trivedi, Phys. Rev. B **91**, 054412 (2015).

[41] G. Chen, R. Pereira, and L. Balents, Phys. Rev. B **82**, 174440 (2010).

[42] I. Zegkinoglou, J. Strempfer, C. S. Nelson, J. P. Hill, J. Chakhalian, C. Bernhard, J. C. Lang, G. Srager, H. Fukazawa, S. Nakatsuji, Y. Maeno, and B. Keimer, Phys. Rev. Lett. **95**, 136401 (2005).

[43] L. Das, F. Forte, R. Fittipaldi, C. G. Fatuzzo, V. Granata, O. Ivashko, M. Horio, F. Schindler, M. Dantz, Yi Tseng, D. E. McNally, H. M. Rønnow, W. Wan, N. B. Christensen, J. Pelliciari, P. Olalde-Velasco, N. Kikugawa, T. Neupert, A. Vecchione, T. Schmitt, M. Cuoco, and J. Chang, Phys. Rev. X **8**, 011048 (2018).

[44] H. Gretarsson, H. Suzuki, Hoon Kim, K. Ueda, M. Krautloher, B. J. Kim, H. Yavaş, G. Khaliullin, and B. Keimer, unpublished.

[45] C. Sow, S. Yonezawa, S. Kitamura, T. Oka, Kazuhiko Kuroki, F. Nakamura, and Y. Maeno, Science **358**, 1084 (2017).

[46] F. Nakamura, M. Sakaki, Y. Yamanaka, S. Tamaru, T. Suzuki, and Y. Maeno, Sci. Rep. **3**, 2536 (2013).